Journal of Ginseng Research 48 (2024) 395–404

Contents lists available at ScienceDirect

Journal of Ginseng Research

journal homepage: www.sciencedirect.com/journal/journal-of-ginseng-research

Research Article

Integration of virtual screening and proteomics reveals potential targets and pathways for ginsenoside Rg_1 against myocardial ischemia

Rongfang Xie [a,1], Chenlu Li [b,1], Chenhui Zhong [a], Zuan Lin [a], Shaoguang Li [a], Bing Chen [a], Youjia Wu [a], Fen Hu [c], Peiying Shi [d,*], Hong Yao [a,e,**]

[a] Department of Pharmaceutical Analysis, School of Pharmacy, Fujian Medical University, Fuzhou, China
[b] Department of Hyperbaric Oxygen, The First Affiliated Hospital, Fujian Medical University, Fuzhou, China
[c] Key Laboratory of Gastrointestinal Cancer (Fujian Medical University), Ministry of Education, Department of Etiology, School of Basic Medical Sciences, Fujian Medical University, Fuzhou, China
[d] Department of Traditional Chinese Medicine Resources and Development, College of Bee Science and Biomedicine, Fujian Agriculture and Forestry University, Fuzhou, China
[e] Fujian Key Laboratory of Drug Target Discovery and Structural and Functional Research, Fujian Medical University, Fuzhou, China

ARTICLE INFO

Keywords:
Myocardial ischemia
Ginsenoside Rg_1
Oxidative stress
Mitogen-activated protein kinase 1
Oxidative phosphorylation
Adenosine kinase

ABSTRACT

Background: Ginsenoside Rg_1 (Rg_1) is one of the main active components in Chinese medicines, *Panax ginseng* and *Panax notoginseng*. Research has shown that Rg_1 has a protective effect on the cardiovascular system, including anti-myocardial ischemia-reperfusion injury, anti-apoptosis, and promotion of myocardial angiogenesis, suggesting it a potential cardiovascular agent. However, the protective mechanism involved is still not fully understood.

Methods: Based on network pharmacology, ligand-based protein docking, proteomics, Western blot, protein recombination and spectroscopic analysis (UV–Vis and fluorescence spectra) techniques, potential targets and pathways for Rg_1 against myocardial ischemia (MI) were screened and explored.

Results: An important target set containing 19 proteins was constructed. Two target proteins with more favorable binding activity for Rg_1 against MI were further identified by molecular docking, including mitogen-activated protein kinase 1 (MAPK1) and adenosine kinase (ADK). Meanwhile, Rg_1 intervention on H9c2 cells injured by H_2O_2 showed an inhibitory oxidative phosphorylation (OXPHOS) pathway. The inhibition of Rg_1 on MAPK1 and OXPHOS pathway was confirmed by Western blot assay. By protein recombination and spectroscopic analysis, the binding reaction between ADK and Rg_1 was also evaluated.

Conclusion: Rg_1 can effectively alleviate cardiomyocytes oxidative stress injury via targeting MAPK1 and ADK, and inhibiting oxidative phosphorylation (OXPHOS) pathway. The present study provides scientific basis for the clinical application of the natural active ingredient, Rg_1, and also gives rise to a methodological reference to the searching of action targets and pathways of other natural active ingredients.

1. Introduction

Cardiovascular diseases (CVDs) caused by multifactorial disorders are regarded as the leading cause of death worldwide owing to its high morbidity, with about 17.9 million deaths each year [1]. Moreover, according to a report by the World Heart Federation, there is an increasing deaths from CVDs than any other cause, and by 2030, there may be 23.6 million deaths per year [2]. Myocardial ischemia (MI) that can lead to myocardial infarction refers to a pathological state where the reduction of blood perfusion in the heart resulting in the decrease of oxygen supply and abnormal myocardial energy metabolism [3]. Although the ischemic myocardium is normally perfused when blood flow is restored, the restoration of oxygenated blood induces a progressive worsening of the ischemic tissue, which is known as

* Corresponding author. Department of Traditional Chinese Medicine Resources and Development, College of Bee Science and Biomedicine, Fujian Agriculture and Forestry University, Fuzhou, 350002, China
** Corresponding author. Department of Pharmaceutical Analysis, School of Pharmacy, Fujian Medical University, Fuzhou 350122, China.
E-mail addresses: peiyshi@126.com (P. Shi), hongyao@mail.fjmu.edu.cn, yauhung@126.com (H. Yao).
[1] These authors have contributed equally to this work.

https://doi.org/10.1016/j.jgr.2024.02.001
Received 25 November 2022; Received in revised form 7 February 2024; Accepted 8 February 2024
Available online 22 February 2024

ischemia/reperfusion injury (I/R) [4,5].

In recent years, traditional Chinese medicine (TCM), a crucial resource of prevention and treatment of cardiovascular diseases, has drawn increasing attention around the world and has broad prospects in MI treatment [6]. Ginsenoside Rg_1 (Rg_1), one of the main components in *Panax ginseng* Meyer and *Panax notoginseng* (Burk.) F.H.Chen, has shown promising therapeutic effects against various cardiovascular system affairs, including myocardial ischemia-reperfusion injury [7], myocardial infarction [8], cardiomyocyte apoptosis, as well as chronic intermittent hypoxia-induced vascular endothelial dysfunction [9]. A research has demonstrated that Rg_1 can interact with Glutathione S-transferase *pi* (GSTP1) to inhibit its mediated S-glutathionylation of OPA1, thereby promoting OPA1-Mitofilin interaction and protecting mitochondrial cristae structure [10]. Lu et al. [11] reported that Rg_1 can alleviate cardiac hypertrophy and fibrosis via the activation of calcineurin pathway and the increase of $[Ca^{2+}]_i$ mediated by calcium sensing receptor, which may be the target of cardioprotection of Rg_1 against myocardial injury. In addition, the recently reported mechanism for Rg_1 against alcohol-induced myocardial injury refers to regulating autophagy and endoplasmic reticulum stress through the AMPK/mTOR and PERK/ATF4/CHOP pathways [12], and Rg_1 can protect against cardiac remodeling via SIRT1/PINK1/Parkin-mediated mitophagy in heart failure [13]. According to these recent research reports, the effect mechanism of Rg_1's anti-MI may involve multiple targets and pathways, which undoubtedly requires more research and understanding.

Currently, proteomics, an application based on high-throughput biotechnologies, is emerging in the identification of all protein expression profiles of cells, tissues, organs or organisms, which provides an unprecedented opportunity for the study of the mechanism of clinical diseases and the discovery of diagnostic markers [14,15]. Proteomics also helps to more comprehensively reveal the functions and mechanisms of complex systems with multiple components, targets, and pathways, such as traditional Chinese medicine (TCM) [16]. The enormous complexity of the proteome, nevertheless, presents a daunting challenge for data analysis. Ligand-based virtual screening aims to screen receptors for a previously known compounds from multiple receptor proteins and explain underlying molecular mechanism of this existing molecule via assessing the combination mode and binding stability between receptor targets and molecules [17]. In view of this, intrinsic complexity of data analysis of proteomics could be reduced by an additional of computer-aided virtual screening.

In the present study, a discovery set of target proteins of Rg_1 for MI was firstly assembled by target fishing. Subsequently, network pharmacology and molecular docking were performed to predict the target proteins and associated pathways of Rg_1 intervention in MI. Simultaneously, differentially expressed proteins (DEPs) for Rg_1 intervening in model of cardiomyocyte injury induced by H_2O_2 were screened using TMT quantitative proteomics at the aids of bioinformatics. Combining the above virtual screening with proteomics results led to the conclusion that Rg_1 might stand up against H_2O_2-induced cardiomyocyte injury partly via targeting mitogen-activated protein kinase 1 (MAPK1) and oxidative phosphorylation pathway. On this basis, the key proteins in the pathway were further verified by Western blot assay. In addition, the utilization of UV and fluorescence spectroscopy demonstrated that adenosine kinase (ADK) could also be regarded as a target for Rg_1 binding and adjusting the oxidative phosphorylation pathway. The present study for the first time discloses the target proteins MAPK1 and ADK, as well as one target pathway oxidative phosphorylation, in part, accounting for the anti-MI effect of Rg_1, which no doubt supplements scientific basis for the clinical application of *P. ginseng*, *P. notoginseng* and Rg_1.

2. Materials and methods

2.1. Materials and reagents

Rg_1 with purity of 98% was purchased from Shanghai Yuanye Bio-Technology Co., Ltd (Shanghai, China), Pierce BCA Protein Assay Kit and TMT Mass Tagging Kit were purchased from ThermoFisher Scientific. Primary antibodies included *p*-ERK, ERK, NDUFS1, UQCRC2, NDUFS4, SDHB and β-Tubulin were obtained from Cell Signaling Technology (Danvers, MA, USA). BL21(DE3)plysS was purchased from Shanghai Cell Bank of Chinese Academy of Science, pET-21a plasmid (ADK) was purchased from Sangon Biotech (Shanghai, China), Isopropyl β-D-1-thiogalactopyranoside DTT, Urea and β-Mercaptoethanol were purchased from Sigma-Aldrich. His-tag purification resin was purchased from Beyotime Biotechnology.

2.2. Virtual screening for potential targets and pathways

The procedures in details can be seen in supplementary materials. Briefly, a target database for Rg_1 intervention in ischemia heart disease was firstly built in this study, followed by "Rg_1-Target-Disease" and "Protein-Protein-Interaction (PPI)" networks construction with the screened target using Cytoscape software [18]. Subsequently, Gene Ontology (GO), Kyoto Encyclopedia of Genes and Genomes (KEGG) pathway, Disease Ontology (DO) enrichment were performed by R packages "clusterProfiler", "topGO" and "DOSE" [19–21], respectively. To investigate the interaction relationship and binding efficiency of putative targets to Rg_1, molecular docking was performed by Sybyl-X 1.3 and Autodock vina, which supplied the precise binding geometry of a ligand–protein complex [22] and the results was visually analyzed using PyMOL view software [23].

2.3. Cell culture and treatment

Rat cardiomyocyte H9c2 cells purchased from Cell bank of Chinese Academy of Sciences (Shanghai, China), were grown in DMEM supplemented with 10% fetal bovine serum (FBS) and 1% penicillin and streptomycin. The cells were maintained at 37 °C in a humidified atmosphere containing 5% CO_2. The cultured media were replaced every 2 days.

2.4. Evaluation of protective effect of Rg_1 on H9c2 cells injured by H_2O_2

H9c2 Cells were seeded in 96-well plates at 1×10^4 cells/well and incubated in 37 °C in 5% CO_2 until cells remained in good growth status. The cells were then pretreated with Rg_1 solutions of different concentration for 24 h, followed by H_2O_2 (200 μM) injury for 2.5 h. Then cell viability conducted by MTT assay was used to evaluate the protective effect of Rg_1 (12.5, 25 and 50 μM) on cardiomyocytes. The absorbance was measured by a microplate reader at 570 nm.

2.5. TMT quantitative proteomics

2.5.1. Generation of protein samples

The experiment was divided into normal cultured cardiomyocytes group (Control group), H_2O_2-induced injury group (Model group), and ginsenoside Rg_1 group (Treatment group). Cells were lysed by sonication with 4 times volume of lysis buffer (8 M urea, 1% protease inhibitor) and centrifuged at 12,000 g for 10 min at 4 °C, and cell debris was removed and supernatant was transferred to a new tube for protein concentration determination using the BCA kit.

The extracted protein was incubated with dithiothreitol (DTT) at a final concentration of 5 mM for 30 min at 56 °C, then alkylated with iodoacetamide at a final concentration of 11 mM for 15 min by light avoidance. The urea concentration of the sample was diluted to less than 2 M. Finally, the protein supernatants were digested overnight with

trypsin (trypsin:protein = 1:50) at 37 °C. Enzymatically lyzed peptides were desalted with Strata X C18 (Phenomenex) and then vacuum freeze dried. The peptides were dissolved with 0.5 M TEAB and labeled according to the TMT kit instructions.

2.5.2. HPLC classification, LC-MS/MS analysis, and bioinformatics analysis

The procedures in details are shown in supplementary materials.

2.6. Western blot assay

In order to validate the predicted pathways enriched from proteomics, Western blot (WB) assay was executed. The samples of denatured proteins were isolated by SDS-PAGE gels, and then transferred onto polyvinylidene fluoride (PVDF) membranes, followed by incubation with primary antibody overnight at 4 °C after being rinsed with 5% nonfat milk and 0.01% Tween-20 in TBST for 2 h at room temperature. Next, the membranes incubated with the HRP-labeled goat anti-rabbit IgG (H&L) antibody for 2 h at room temperature. Finally, target proteins were detected using enhanced chemiluminescence (ECL).

2.7. Spectral analysis

2.7.1. ADK protein preparation

2.7.1.1. Cloning and expression of adenosine kinase. Nucleotide sequence (NCBI Reference Sequence: NM_001123.4) of adenosine kinase (ADK) coding for 345 amino acids were cloned in pET-21a expression vector with *Bam*HI and Xhol restriction sites. The resulting recombinant was transformed into competent BL21(DE3) pLysS host *E. coli* cells. Positive colonies on agar plates containing ampicillin were screened and validated. Cells were grown in modified LuriaBertani (LB) media containing 100 μg/mL ampicillin. The expression of protein was induced by addition of 0.4 mM IPTG at 16 °C for 10 h. Next, induced cells were harvested by centrifugation at 4000*g* for 20 min.

2.7.1.2. Purification and SDS-PAGE analysis of the recombinant ADK. The collected cells were re-suspended with lysis buffer and crushed by ultrasonic. After centrifugation at 15,000 g and 4 °C for 10 min, the supernatant was discarded and the inclusion body pellet was washed with detergent washing buffer and then dissolved in denatured solution. Obtained supernatant was filtered with a 0.22 μm filter membrane before purified by Ni-affinity chromatography. After washing off the miscellaneous proteins, ADK protein was eluted using a buffer containing imidazole. The purity of recombinant ADK was checked by SDS-PAGE and its concentration was determined by the BCA assay.

2.7.2. Analysis of UV–vis and fluorescence spectra

To investigate whether ADK protein and Rg_1 interact with each other, UV–Vis and fluorescence spectra were recorded separately at 25 °C after the resulting ADK protein solution was incubated with different concentrations of Rg_1 at 4 °C for 2 h. UV–Vis spectra were measured by Agilent Cary 60 UV–Vis spectrophotometer using with the scanning wavelength from 250 to 450 nm. Fluorescence spectra were detected using the Agilent Cary Elipse fluorescence spectrophotometer. The spectral resolution was 1.0 nm.

2.8. Statistical analysis

All data were expressed as mean ± SD and analyzed using the SPSS 18.0. Statistical comparisons between groups were made via one-way ANOVA. Differences were considered significant when $p < 0.05$.

3. Results and discussion

3.1. Virtual screening

The chemical structure of Rg_1 is shown in Supplementary Fig. S1A. From target fishing and, 121 proteins or genes were screened as potential targets for Rg_1 against CVDs. The resulting database was shown in Supplementary Table S1.

3.1.1. "Rg_1-Targets-Disease" and "PPI" network analysis

The 121 intersecting target proteins were fed into the DAVID server (https://david.ncifcrf.gov/) to obtain relevant disease information, and construct the "Rg_1-Targets-Disease" network. As shown in Supplementary Fig. S1B, the V shape node in the network represents Rg_1, the diamonds show various diseases and the circles represent the potential target genes associated with the diseases. The network consists of 92 nodes and 402 edges, including 83 target gene nodes, 8 disease nodes and 1 component node, with larger nodes representing larger degree. High-degree nodes (Degree >5), including NOS3, ERS1, VEGFA, MMP3, PPARG, PPARA, ADH1C, GSTP1, IGF1 and ESR2, exhibited highly associated with CVD diseases, such as atherosclerosis and hypertension.

PPI network with 117 target gene nodes and 1486 edges is as shown in Supplementary F. 1C after hiding the targets without interaction. ALB, MAPK1, EGFR, SRC, ESR1, MAPK8, HSP90AA1, IGF1 and CASP3 were considered as the key hubs in this network according to the degree value analysis (Degree >40), and their related information is shown in Supplementary Table S2.

3.1.2. GO, KEGG and DO enrichment analysis of potential targets

GO enrichment analysis was shown in Fig. 1A. For BP entries, they involve in the cellular response to oxidative stress and reactive oxygen species, regulation of MAP kinase activity, etc. For CC entries, they are mainly related to transcription factor complex, blood microparticle, membrane domain, membrane rafts, *etc*. Entries on MF were enriched including protein serine/threonine kinase activity, fatty acid binding, hormone binding, monocarboxylic acid binding, carboxylic acid binding, *etc*.

DO enrichment analysis is a tool to annotate genes from a disease perspective and understand disease pathogenesis based on genes. The intersection genes were mainly enriched in coronary artery disease, cancers such as connective tissue cancer, breast carcinoma and bone cancer, as well as obesity (Fig. 1B). Top 10 KEGG pathways ranked were shown in Fig. 1C, primarily involving the Reactive oxygen species, FoxO signaling pathway, MAPK signaling pathway, Proteoglycans in cancers, Atherosclerosis, *etc*.

According to the GO, KEGG and DO enrichment analysis, it seems that oxidative stress, reactive oxygen species, and MAP kinase activity are important relative issues for Rg_1 against CVDs due to their high occurrence frequency in the genes annotation. These also suggest that an oxidative stress injury model may be suitable in the investigation of effect and mechanism of Rg_1 against CVDs.

3.1.3. Molecular docking results

The binding of Rg_1 to 121 intersecting target proteins from virtual screening were assessed with the index, Total Score and Binding energy provided by Sybyl 1.3 and AutoDock Vina, respectively. A total of 19 high scoring proteins including PAH, MAPK1, DAPK1, MMP8, PYGL, ADK, *etc*. were screened with Total Score >5.0 and binding energy ≤ −7 kcal/mol, suggesting that these proteins could have binding activity to Rg_1. The docking results were shown in Fig. 2A and Supplementary Table S3. Especially, the four proteins, phenylalanine-4-hydroxylase (PAH), complement factor B (CFB), MAPK1, and ADK had the most stable binding conformation to Rg_1 (Total Score ≥8 and Binding energy ≤ −7.5 kcal/mol). As shown in Fig. 2B, the amino acid residues binding with Rg_1 in the PAH protein are HIS-285 (2.5 Å), TYR-377 (2.6 Å and 3.2 Å), and THR-278 (2.4 Å and 2.8 Å) with five hydrogen bonds. The

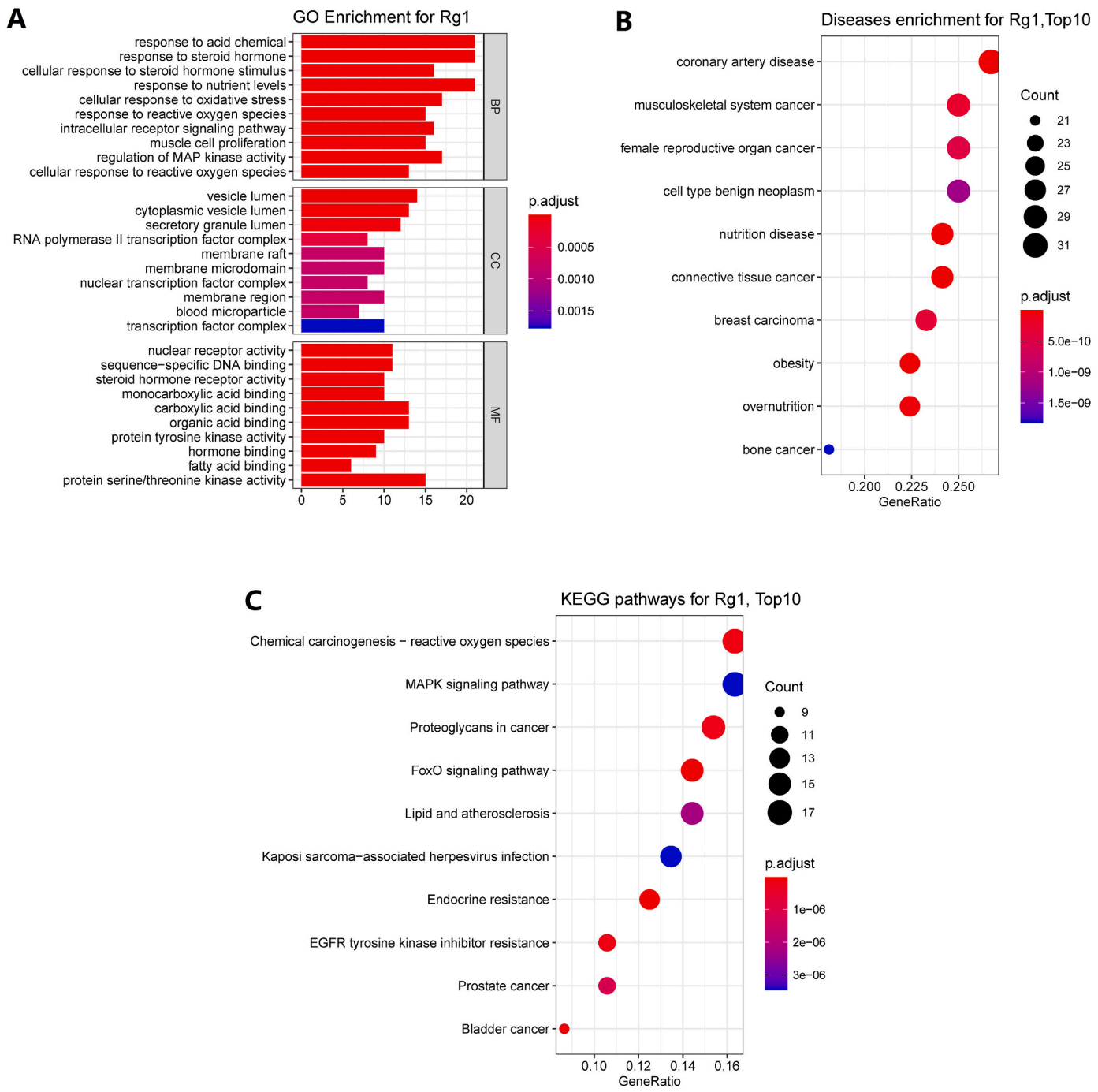

Fig. 1. Enrichment analysis of potential targets. (A) GO enrichment. (B) DO enrichment (C) KEGG pathway enrichment.

residues TYR-172B (2.4 Å) and HIS-39 (2.6 Å) in the CFB protein bind to Rg_1, forming two hydrogen bonds. The residues in the ADK protein interacting with Rg_1 are LEU-40 (3.5 Å) and GLN-38 (3.5 Å) with two hydrogen bonds. MAPK1 protein has more amino acid residues that interact with Rg_1, including MET-108 (2.4 Å), ASP-167 (2.4 Å), ARG-67 (2.8 Å, 3.3 Å and 3.4 Å) and ASP-149 (2.3 Å) with six hydrogen bonds.

PAH, a tyrosine oxygenase mainly existing in liver is involved in phenylalanine metabolism. A high ratio of phenylalanine to tyrosine (Phe/Tyr) is often related to immune activation and inflammatory responses [24]. CFB is mainly synthesized by hepatocytes and macrophages and is an important component involved in complement activation. Increased CFB levels can be seen in cardiovascular disease, type 2 diabetes and malignancies, while autoimmune disease, liver cirrhosis and acute glomerulonephritis result in decreased levels of this gene [25]. ADK is an abundant enzyme in mammalian tissues that catalyzes the transfer of γ-phosphate from ATP to adenosine (ADO) and is involved in the regulation of extracellular ADO and intracellular adenine nucleotide concentrations. Inhibiting ADK could raise the intra- and extra-cellular concentrations of ADO, which has extensive protective effects in the cardiovascular system including prevention or reduction of inflammation, promotion of neovascularization and ischemic preconditioning leading to increasing oxygen supply [26,27]. MAPK1 (ERK2), a member of MAP kinase family also known as extracellular signal-regulated kinases (ERKs) whose phosphorylation can cause cardiac hypertrophy, is an integration point for a variety of biochemical signals and involved in a variety of cellular processes such

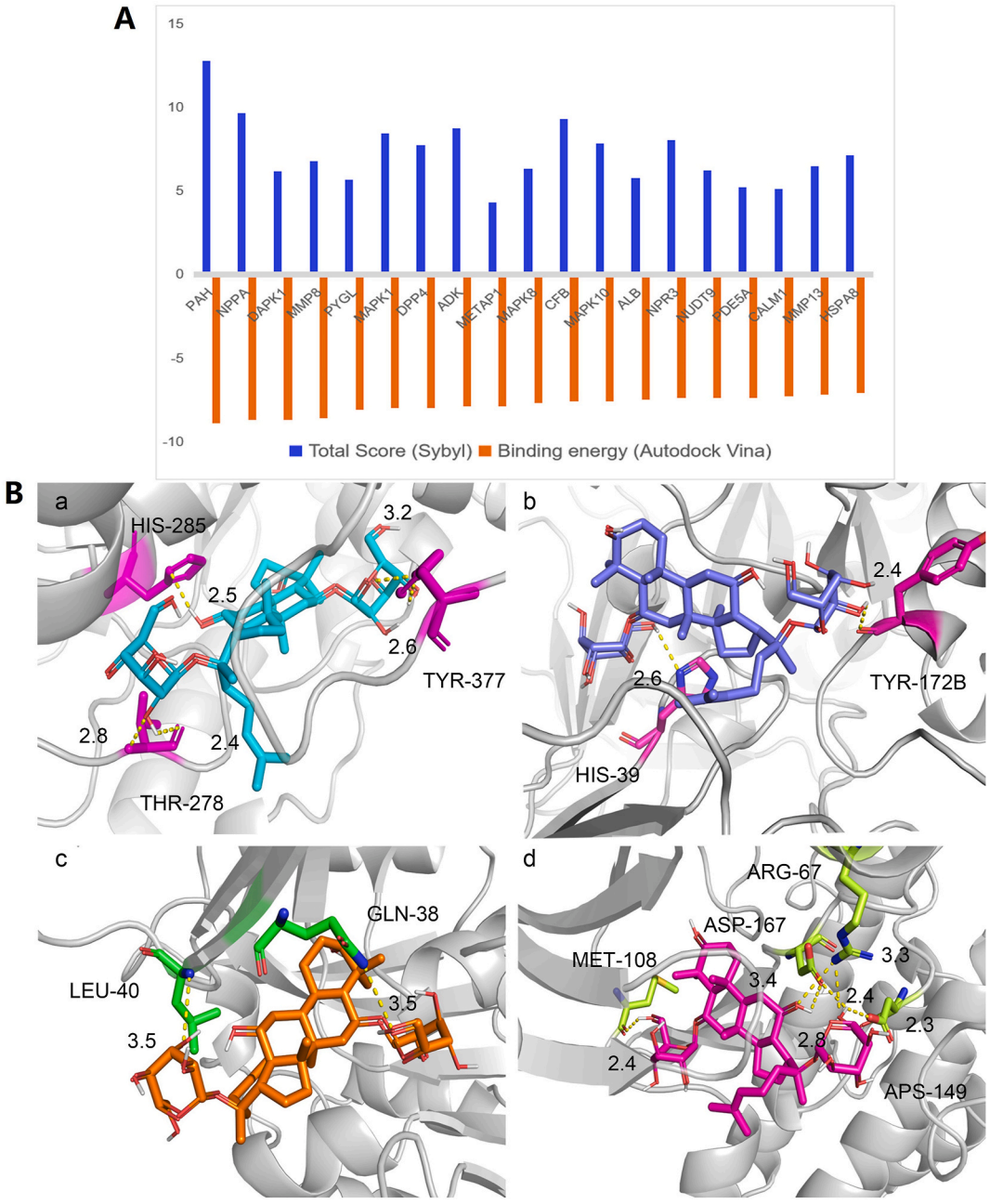

Fig. 2. Structure-based prediction of Rg1 protein interactions. (A) Proteins with strong binding activity to Rg_1 evaluate by Total Score and binding energy. (B) Visualization of proteins interacting with Rg_1 (a: PAH; b: CFB; c: ADK; d: MAPK1).

as cell proliferation, differentiation and transcription [25,27].

According to these results, it is concluded that the four proteins, PAH, CFB, MAPK1 and ADK could be the potential binding targets for Rg_1. Especially, ADK and MAPK1 could possess close correlation to therapeutic effect of Rg_1 against CVDs.

3.2. *Protection of Rg_1 against H_2O_2-induced cardiomyocytes injury*

Based on the above virtual screening results, the H_2O_2-induced oxidative injury model of cardiomyocytes was used in the test. Different concentrations of H_2O_2 (100, 150, 200, 250 and 300 μM) were added to normal cultured H9c2 cells for 2.5 h. The cell viability decreased gradually with the increasing H_2O_2 concentration. As shown in Fig. 3A (a), under the treatment of 150 μM H_2O_2, cell viability still maintained more than 75% compared with the normal control group. But the viability was significantly reduced to about 50% when the H_2O_2 concentration reached 200 μM, indicating the success of the oxidative stress injury model. Therefore, 200 μM H_2O_2 treatment for 2.5 h was used to simulate oxidative stress injury in H9c2 cells. To examine the possible toxicity of Rg_1 on normal cultured H9c2 cells, graded concentrations of Rg_1 solution (6.25, 12.5, 25, 50, 100 and 200 μM) were added to H9c2 cells for 24 h and cell viability was examined (Fig. 3A(b)). The results indicated that Rg_1 did not generate any effect on the growth of H9c2 cells within the concentration range from 6.25 to 200 μM. As shown in Fig. 3A(c), the survival rate of the intervention group cells injured by H_2O_2 with Rg_1 at 12.5, 25 and 50 μM is significantly increased to 54.42%, 55.32% and 58.24%, respectively compared to 43.50% in model group, indicating that Rg_1 has a protection against H_2O_2-induced cardiomyocyte injury.

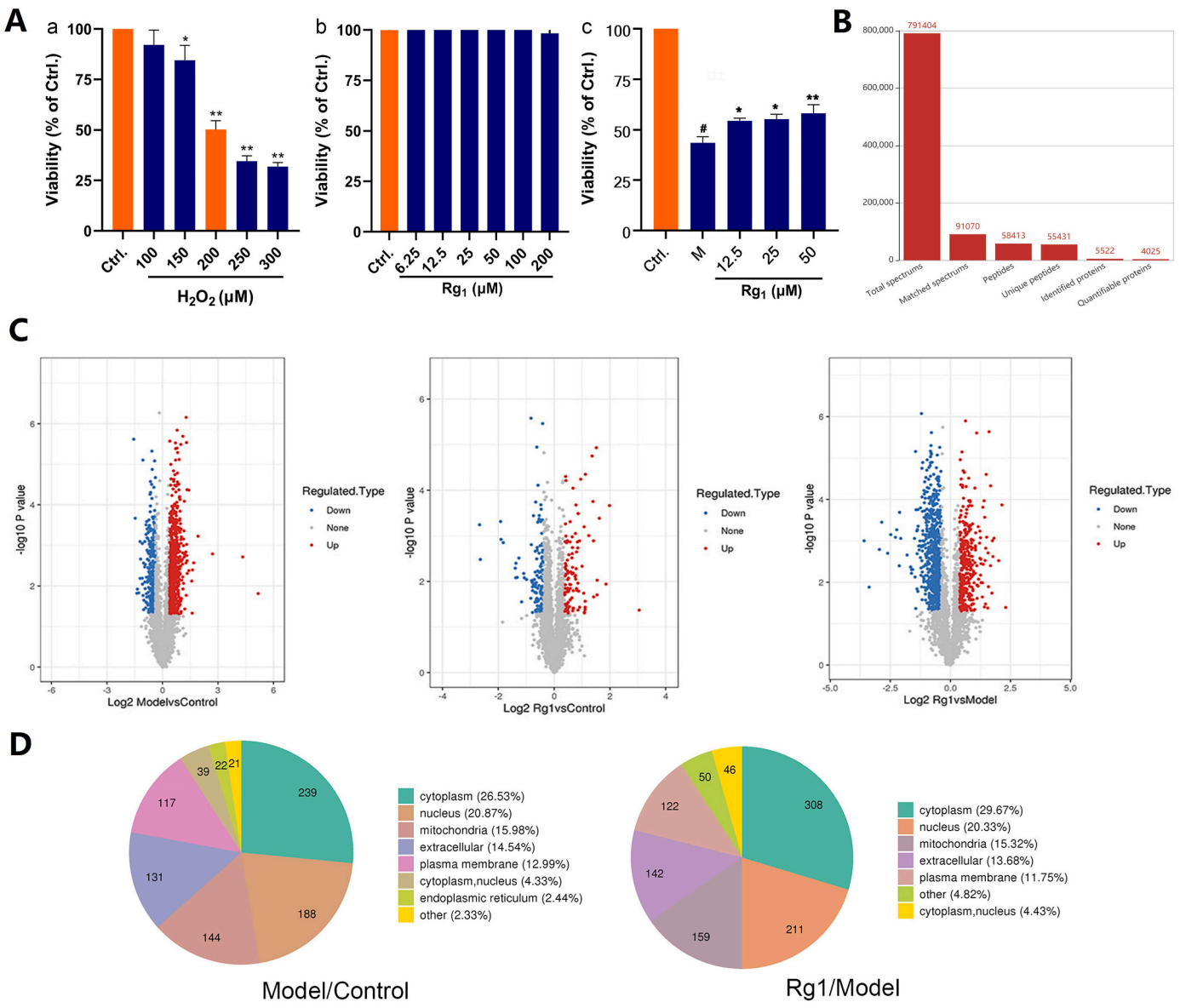

Fig. 3. (A) MTT assay. (a) Concentration screening of H_2O_2 induced H9c2 cardiomyocyte injury (mean ± SD, n = 3). *$p < 0.001$ and **$p < 0.0001$, vs. the control group. (b) Cytotoxicity of Rg_1 on H9c2 cell (mean ± SD, n = 3). (c) Effect of Rg_1 on H9c2 cell viability after treatment with H_2O_2. ##$p < 0.01$ vs. the control group; *$p < 0.05$ and **p < 0.01, vs. the model group (mean ± SD, n = 3). $^{\#}p < 0.001$, vs. Control group; *$p < 0.001$, **$p < 0.0001$, vs. the model group. (B) Statistical chart of mass spectrum data. (C) The volcano diagrams of DEPs ($p < 0.05$, |Fold Change| > 1.3). Red and green points represent up- and down-regulated proteins respectively. (D) Classification of subcellular structural localization of DEPs.

3.3. Quantitative proteomics for Rg_1 intervention on cardiomyocytes injured by H_2O_2

3.3.1. Protein identification overview

As shown in Fig. 3B, a total of 791,404 secondary spectra were obtained from the mass spectrometry analysis. After searching the protein theoretical data library, 91,070 valid secondary spectra were available, giving a spectrum utilization rate of 11.5%. The number of peptides with specificity was 55,431 out of a total of 58,413 peptides. 5522 proteins were identified, of which 4025 could be used for quantification.

A change in differential expression of more than 1.3 is as the threshold of change for significant up-regulation, and less than 1/1.3 is as the threshold of change for significant down-regulation (p-value <0.05). The number of differentially expressed proteins (DEPs) in the different groups was shown in Fig. 3C. There are 901 DEPs in the model group compared to the control, of which 587 proteins are up-regulated and 314 proteins are down-regulated, indicating a significant change in the level of protein expressed after H_2O_2 injury and the successful establishment of a damage model. Of the 1038 DEPs in the Rg_1 intervention group compared to the model, 346 proteins are up-regulated and 692 proteins are down-regulated. It was shown that the expression of the proteins in cardiomyocytes interfered by H_2O_2 altered again in the presence of Rg_1, suggesting the possible protection of Rg_1 on the cells.

The subcellular structural localization of DEPs is shown in Fig. 3D. DEPs between the model and normal groups account for 26.53% in the cytoplasm, 20.87% in the nucleus, 15.98% in the mitochondria and 14.54% in the extracellular region. DEPs between the Rg_1-treated and model groups account for 29.67% in the cytoplasm, 20.33% in the nucleus, 15.32% in the mitochondria and 13.68% in the extracellular region. A large number of proteins differ in the cytoplasm, nucleus and mitochondria between groups, suggesting that the mechanism of H_2O_2 injury on cardiomyocytes as well as Rg_1 protection on the ischemic cardiomyocyte model, could mainly involve the functions of the

cytoplasm, nucleus and mitochondria.

3.3.2. Bioinformatics analysis of DEPs

GO enrichment analysis was performed on DEPs among groups. As shown in Fig. S2 (A) of supplementary materials, compared with control group, it can be seen that H_2O_2 injury affect the BP of cardiomyocytes, mainly referring to up-regulating tricarboxylic acid metabolic process, nucleoside biophosphate metabolic process and aerobic respiration and down-regulating actin filament bundle organization and regulation of protein complex disassembly. Compared with the H_2O_2 injury and control group, Rg_1 treatment recovers the above affected processes to normal cardiomyocyte level, and especially, Rg_1 significantly affects the BPs, including down-regulating ATP synthesis coupled electron transport and up-regulating pyridine nucleotide metabolic process, nicotinamide nucleotide metabolic process and oxidoreduction coenzyme metabolic process. For MF analysis, as shown in supplementary Fig. S2 (B) in supplementary materials, Rg_1 treatment almost reverses all the affected molecular functions due to the H_2O_2-induced injury and significantly down-regulates the NADH dehydrogenase activity and oxidoreductase activity compared to H_2O_2 injury group. In addition, CC analysis also showed that Rg_1 reverses all the affected cellular components due to the H_2O_2-induced injury (supplementary Fig. S2 (C)).

The KEGG pathway enrichment analysis is shown in Fig. 4, which reveals that Rg_1 exerts multi-target and multi-pathway anti-MI effects mainly through the signaling pathways such as oxidative phosphorylation (OXPHOS), Parkinson and Alzheimer's diseases, citrate cycle (TCA) etc.

Based on the above bioinformatics analysis, the intervention mechanism of Rg_1 on H_2O_2 induced myocardial cell injury is at least partially directed towards inhibiting ATP synthesis, NADH dehydrogenase activity, and oxidoreductase activity, thereby slowing down the energy metabolism pathways of myocardial cells, such as oxidative phosphorylation and TCA.

3.4. Effect of Rg_1 intervention on the key proteins of MAPK and oxidative phosphorylation pathway

MAPK1/ERK2 and MAPK3/ERK1 as two MAPKs play important roles in the MAPK/ERK cascade. Research has shown that cell survival and proliferation are regulated by the ERK signaling pathway, which activation can reduce MI injury in focal ischemia-reperfusion models [27]. On the contrary, inhibition of ERK signaling can alleviate organ dysfunction. In this study, MAPK1 (Uniport ID: P28438) was identified as one key target of Rg_1 intervention on MI by virtual screening and proteomics assay, and was therefore validated at the protein level. As shown in Fig. 5, the concentration-dependent reduction of ERK (Uniport

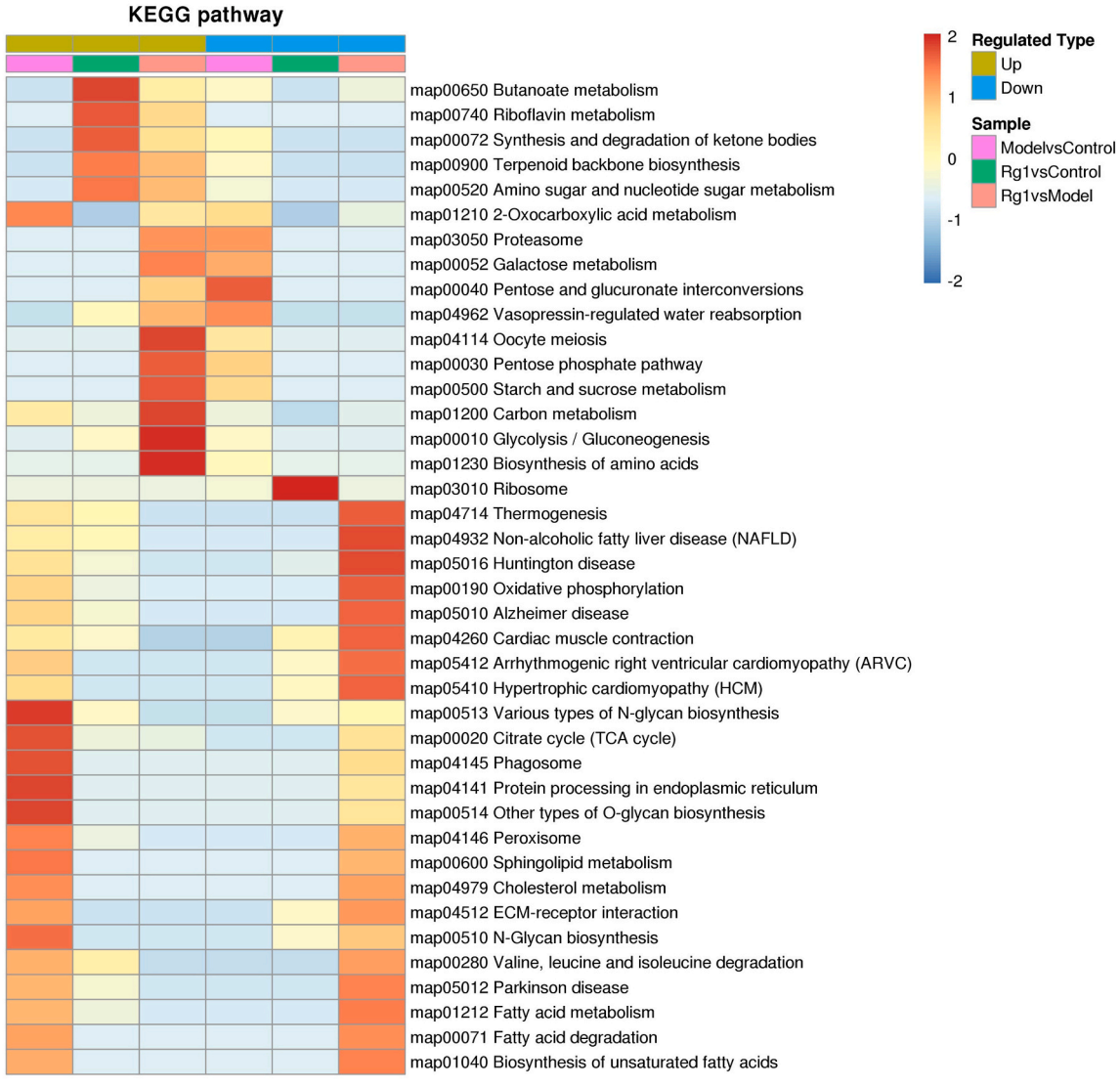

Fig. 4. KEGG Enrichment analysis of DEPs from TMT quantitative proteomics for Rg_1 treatment of H9c2 cardiomyocytes injured by H_2O_2.

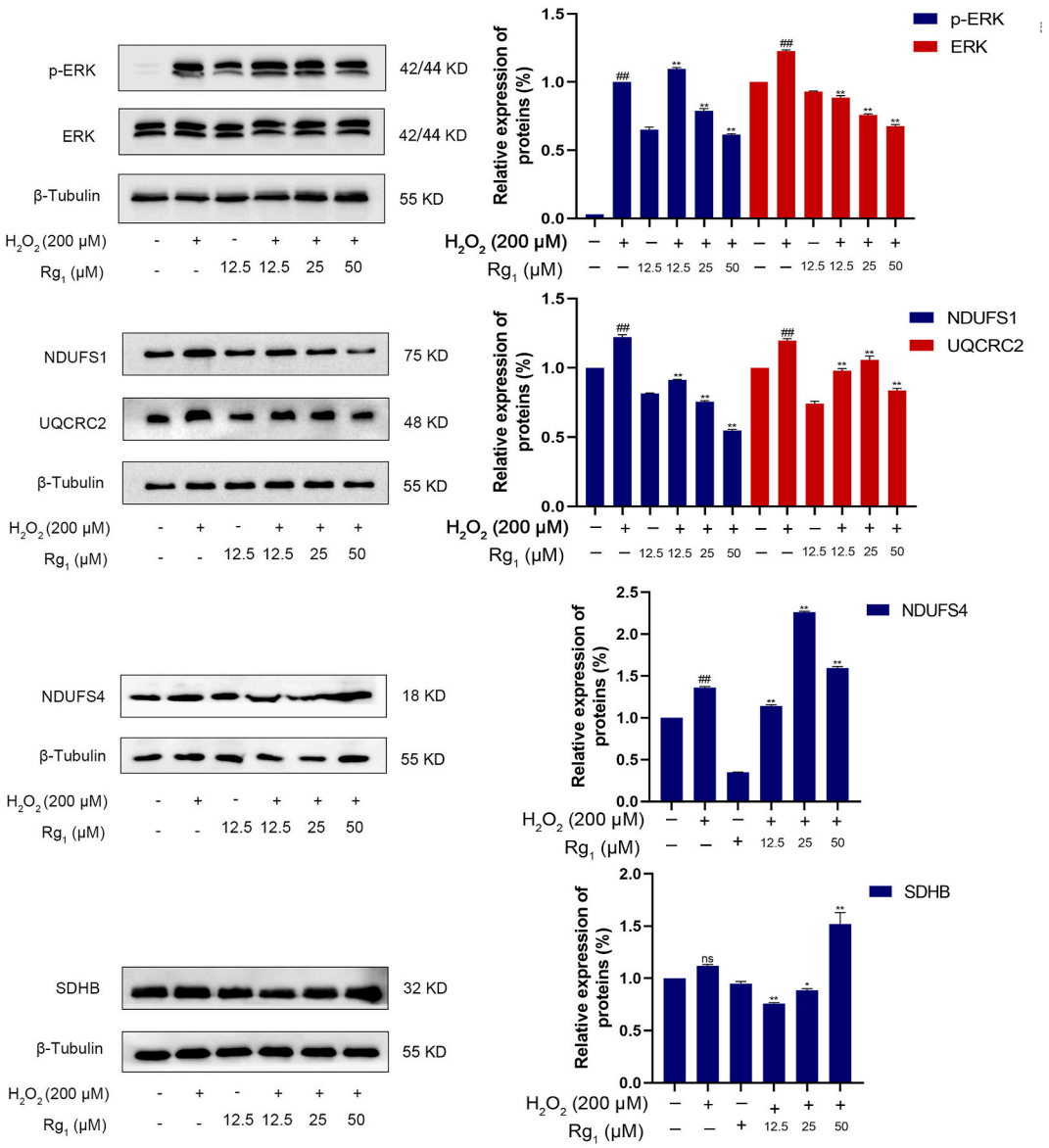

Fig. 5. Rg_1 decreased phosphorylation and activation on MAPK and oxidative phosphorylation pathway. (A) Effects of Rg1 on expression of MAPK1. (B, C, D) Effects of Rg1 on expression of NDUFS1, UQCRC2, NDUFS4, SDHB in H9c2. Values are mean ± SEM, n = 3; #$p < 0.05$, ##$p < 0.01$, vs. Control; *$p < 0.05$, **$p < 0.01$, vs. Model. ANOVA.

ID: P27361 and P28438) by Rg_1 was significant, while the reduction of *p*-ERK was observed at 25 μM and 50 μM.

OXPHOS refers to the synthesis of ATP from ADP and inorganic phosphate by transferring the free energy released during biological oxidation. It is the main source of energy for life-sustaining activities in aerobic cells, including electron transfer and phosphorylation. The present proteomics study has disclosed OXPHOS is one of the main action pathways for Rg_1 against the oxidative injury. The electron transport chain consists of complex I (NADH oxidase, NOX), complex II (Succinate dehydrogenase, SDH), complex III (Cytochrome C oxidoreductase), complex IV (Cytochrome C oxidase) and complex V (ATP synthase) [28,29]. Among them, Complex I and complex III are two important sites for the production of Reactive Oxygen Species (ROS) by oxidative stress, and complex I may be the main source of ROS production in mammalian mitochondria [30–32]. Oxidative stress was one of the most dominant processes of Rg_1 intervention in MI from virtual screening assay. Therefore, it is necessary to investigate the effect of Rg_1 on the OXPHOS signaling pathway in H_2O_2-injured cardiomyocytes by measuring the levels of protein complex I (NDUFS1, NDUFS4), complex II (SDHB), complex III (UQCRC2) and complex IV (COX5A) by Western blot technique. As shown in Fig. 6, Rg_1 significantly down-regulates the expression of NDUFS1 and UQCRC2, with a concentration-dependent inhibition in NDUFS1. The levels of NDUFS4 and SDHB are reduced at low concentrations of Rg_1, but increased at higher concentrations, suggesting that Rg_1 might only inhibit the OXPHOS at lower concentrations.

According to the above results, MAPK1 can be considered as a key protein in the inhibition of H_2O_2-induced cardiomyocyte injury by Rg_1. Meanwhile, in OXPHOS pathway, Rg_1 mainly inhibited the expression of complex I (NDUFS1 et al.) and complex III subunits (UQCRC2 et al.) and promoted complex II (SDHB et al.) to reduce H_2O_2-induced oxidative stress in H9c2. It can be assumed that Rg_1 inhibits H_2O_2-induced oxidative stress by down-regulating the expression of subunits of complex I and complex III, thereby reducing the production of ROS and promoting the expression of subunits of complex II to catalyze the oxidation of succinate to ferredoxin, which ensure the electron transport chain equipped to produce ATP and prevent cells from dying due to lack of energy.

In addition, more experimental evidence is needed to prove whether

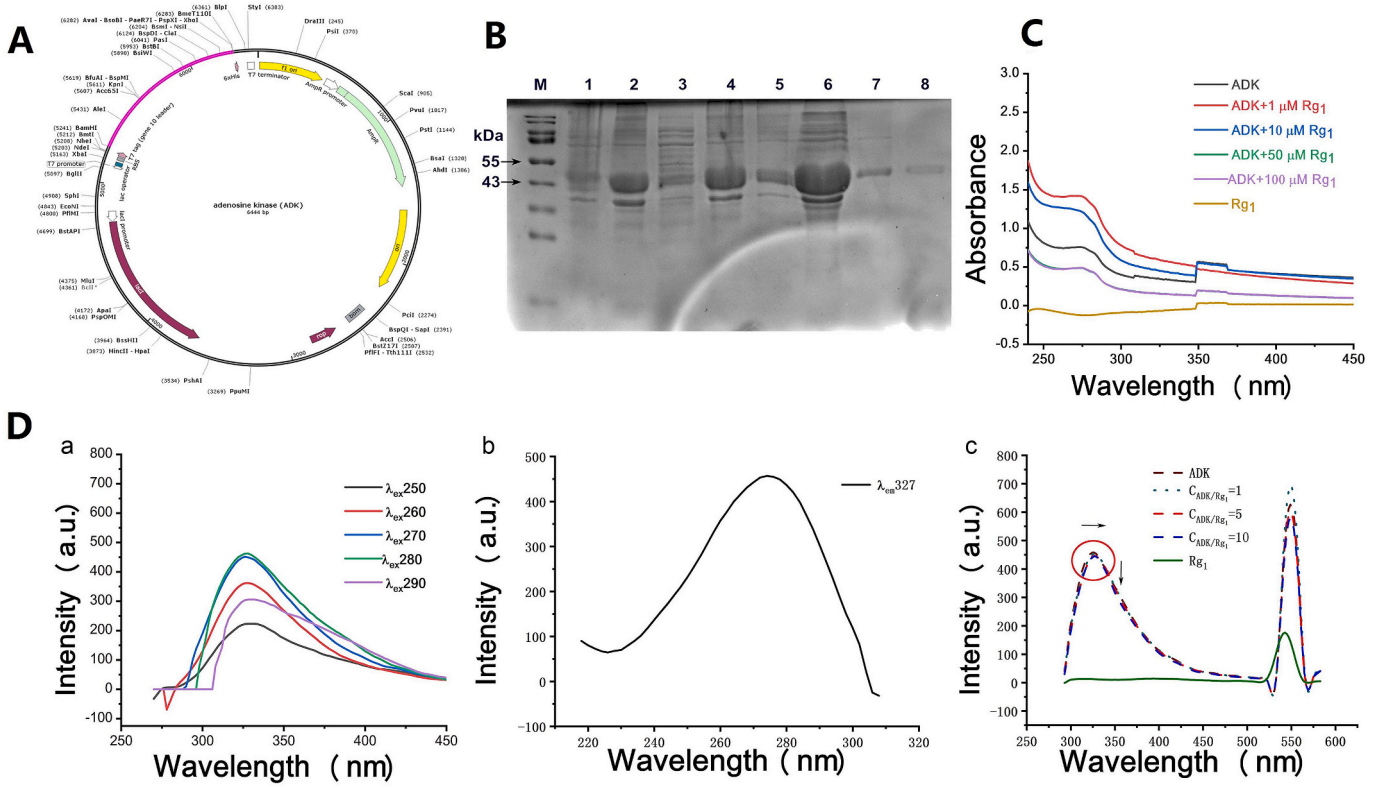

Fig. 6. The interaction between ADK and different concentration of Rg_1. (A)Plasmid map. (B) Purification and characterization of the recombinant ADK. Lanes: M, molecular mass markers; 1, precipitation of *E. coli* cells; 2, precipitation of the lysed cells; 3, supernatant of the lysed cells; 4, precipitation of the lysed cells after washing with buffer; 5, Pellet of dissolved in 6 M urea; 6, Supernatant of dissolved in 6 M urea; 7,8, purified target ADK. (C) The UV/Vis absorption spectra of ADK in the presence of different concentration Rg_1 (1, 10, 50, 100 μM). (D) Fluorescence spectra of ADK. (a) Emission spectra of ADK at different excitation wavelengths. (b) Absorption spectrum of ADK with a fixed emission wavelength of 327 nm. (c) Emission spectra of ADK with Rg_1 at different concentration ratios with a fixed excitation wavelength of 274 nm.

Rg_1 inhibits OXPHOS pathway by targeting MAPK1 in the future. E.g., isoproterenol (ISO)-induced and left anterior descending (LAD) ligation-induced MI murine model may be used to validate the effect of Rg_1 on the regulation of the MAPK1 and its downstream protein expression and OXPHOS pathway. On this basis, gene edited animal models such as MAPK1 knockdown (MAPK1 (−/−)) mice should be constructed and used to evaluate the relationship of MAPK1 with the OXPHOS pathway, and further confirm the targeted effects of Rg_1 on the MAPK1 and OXPHOS pathways in MI animal models with MAPK1 knockdown.

3.5. *Spectral properties of Rg_1 toward ADK*

According to the virtual screening results, ADK is considered as one potential binding target for Rg_1. To confirm that a reaction between ADK and Rg_1 does really occur, ADK protein recombination and purification were carried out and the spectral properties of Rg_1 toward ADK were investigated.

The gene sequence and plasmid map of ADK are shown in Fig. 6A. Recombinant protein ADK was eluted with imidazole buffer and identified by SDS-PAGE to have a molecular weight of about 45 kDa (Fig. 6B). The benzene rings of tyrosine, phenylalanine and tryptophan residues in protein molecules contain conjugated double bonds that give the proteins their UV-absorbing properties. Protein structure is altered and its UV spectrum changes accordingly when a small molecule enters a protein. Fluorescence spectroscopy is another method for studying the interaction of a small molecule ligand with its receptor protein, as well as a substrate with an enzyme. Hence, the structural change of ADK (0.26 μM) upon addition of Rg_1 was explored by measuring UV–Vis absorption and fluorescence spectra in a buffer solution containing imidazole (pH = 8.0). Fig. 6C shows the differed UV-absorption intensities in the presence of different concentrations of Rg_1 with a maximum absorption wavelength at about 274 nm. As shown in Fig. 6D, the emission spectra of ADK were detected by setting the excitation wavelength in the 250–290 nm range. Maximum emission of ADK occurred at wavelength 327 nm. The absorption spectrum of ADK was then obtained by fixing the emission wavelength at 327 nm, and the optimum excitation wavelength was 274 nm. Finally, we used 274 nm as the excitation wavelength to scan the spectra of ADK with Rg_1 at different concentration ratios. The fluorescence intensity of ADK decreased with increasing concentration of Rg_1, and the position of the maximum emission peak of fluorescence was red-shifted ($\Delta\lambda = 2$ nm).

According to the above results, it can be concluded that ADK can interact with Rg_1. In fact, ADK is a critical regulator of adenosine function and it can catalyze phosphorylation of extracellular adenosine to 5′-adenosine-monophosphate (AMP). Several studies have reported good attenuation of regional MI by administration of an ADK inhibitor, iodotubercidin, and the protection by ADK inhibitors was mediated via inhibition of ROS [33,34]. It is therefore highly likely that ADK is the target of Rg_1, inhibiting the action of ADK catalyzing adenosine and causing an increase in extracellular adenosine concentration. To confirm the role of ADK for Rg_1 exerting its therapeutic effect against CVDs, further research should be conducted using MI models with ADK knockdown animals in the future.

4. Conclusion

In this paper, a strategy combining network pharmacology, ligand-based protein docking, proteomics, Western blot, protein recombination and spectroscopic analysis (UV–Vis and fluorescence spectra) techniques has been carried out for screening potential targets and

pathways of Rg_1 against MI. It is proved that oxidative stress is a primary cellular response in MI and Rg_1 can effectively alleviate H_2O_2-induced oxidative stress in H9c2 cardiomyocytes, partly via targeting MAPK1 (ERK2) and ADK, and inhibiting OXPHOS pathway. The present study undoubtedly adds scientific basis into the clinical application of the natural active ingredient, Rg_1, and also provides methodological reference to the searching of action targets or pathways of other natural active ingredients.

Declaration of competing interest

The authors declare no conflict of interest.

Acknowledgements

This work was supported by National Natural Science Foundation of China (81973558), key project supported by the Natural Science Foundation of Fujian province, China (2021J02033), and the Funds of Fujian Key Laboratory of Drug Target Discovery and Structural and Functional Research, Fujian Medical University, China (FKLDSR-202104).

Appendix A. Supplementary data

Supplementary data to this article can be found online at https://doi.org/10.1016/j.jgr.2024.02.001.

References

[1] Benjamin EJ, Blaha MJ, Chiuve SE, Cushman M, Das SR, Deo R, De Ferranti SD, Floyd J, Fornage M, Gillespie C. Heart disease and stroke statistics—2017 update: a report from the American Heart Association. Circulation 2017;135(10):e146–603.
[2] Mozaffarian D, Benjamin EJ, Go AS, Arnett DK, Blaha MJ, Cushman M, Das SR, De Ferranti S, Després J-P, Fullerton HJ. Heart disease and stroke statistics—2016 update: a report from the American Heart Association. Circulation 2016;133(4):e38–360.
[3] Marzilli M, Crea F, Morrone D, Bonow RO, Brown DL, Camici PG, Chilian WM, DeMaria A, Guarini G, Huqi A. Myocardial ischemia: from disease to syndrome. Int J Cardiol 2020;314:32–5.
[4] Yellon DM, Hausenloy DJ. Myocardial reperfusion injury. N Engl J Med 2007;357(11):1121–35.
[5] Forman MB, Virmani R, Puett DW. Mechanisms and therapy of myocardial reperfusion injury. Circulation 1990;81(3 Suppl):69–78.
[6] Chen K, Li G, Geng F, Zhang Z, Li J, Yang M, Dong L, Gao F. Berberine reduces ischemia/reperfusion-induced myocardial apoptosis via activating AMPK and PI3K–Akt signaling in diabetic rats. Apoptosis 2014;19(6):946–57.
[7] Li L, Pan C-S, Yan L, Cui Y-C, Liu Y-Y, Mu H-N, He K, Hu B-H, Chang X, Sun K. Ginsenoside Rg1 ameliorates rat myocardial ischemia-reperfusion injury by modulating energy metabolism pathways. Front Physiol 2018;9:78.
[8] Wang X-d, Gu T-x, Shi E-y, Lu C-m, Wang C. Effect and mechanism of panaxoside Rg1 on neovascularization in myocardial infarction rats. Chin J Integr Med 2010;16(2):162–6.
[9] Zhao F, Lu ML, Wang HX. Ginsenoside Rg1 ameliorates chronic intermittent hypoxia-induced vascular endothelial dysfunction by suppressing the formation of mitochondrial reactive oxygen species through the calpain-1 pathway. J Gin Res 2023;47(1):144–54.
[10] Zhu HM, Yan CY, Yao P, Li P, Li Y, Yang H. Ginsenoside Rg1 protects cardiac mitochondrial function via targeting GSTP1 to block S-glutathionylation of optic atrophy 1. Free Radical Biol Med 2023;204:54–67.
[11] Lu ML, Wang J, Sun Y, Li C, Sun TR, Hou XW, Wang HX. Ginsenoside Rg1 attenuates mechanical stress-induced cardiac injury via calcium sensing receptor-related pathway. J Gin Res 2021;45(6):683–94.
[12] Tian G, Li J, Zhou LN. Ginsenoside Rg1 regulates autophagy and endoplasmic reticulum stress via the AMPK/mTOR and PERK/ATF4/CHOP pathways to alleviate alcohol-induced myocardial injury. Int J Mol Med 2023;51(1):56.
[13] Guan SB, Xin YF, Ding YG, Zhang QL, Han W. Ginsenoside Rg1 protects against cardiac remodeling in heart failure via SIRT1/PINK1/Parkin-mediated mitophagy. Chem Biodivers 2023;20(2):e202200730.
[14] Cheung CHY, Juan H-F. Quantitative proteomics in lung cancer. J Biomed Sci 2017;24(1):1–11.
[15] Xu M, Deng J, Xu K, Zhu T, Han L, Yan Y, Yao D, Deng H, Wang D, Sun Y. In-depth serum proteomics reveals biomarkers of psoriasis severity and response to traditional Chinese medicine. Theranostics 2019;9(9):2475.
[16] Lam MP, Ping P, Murphy E. Proteomics research in cardiovascular medicine and biomarker discovery. J Am Coll Cardiol 2016;68(25):2819–30.
[17] Klebe G. Virtual ligand screening: strategies, perspectives and limitations. Drug Discov Today 2006;11(13–14):580–94.
[18] Shannon P, Markiel A, Ozier O, Baliga NS, Wang JT, Ramage D, Amin N, Schwikowski B, Ideker T. Cytoscape: a software environment for integrated models of biomolecular interaction networks. Genome Res 2003;13(11):2498–504.
[19] Yu G, Wang L-G, Han Y, He Q-Y. clusterProfiler: an R package for comparing biological themes among gene clusters. OMICS 2012;16(5):284–7.
[20] Yu G, Wang L-G, Yan G-R, He Q-Y. DOSE: an R/Bioconductor package for disease ontology semantic and enrichment analysis. Bioinformatics 2015;31(4):608–9.
[21] Carlson M, Falcon S, Pages H, Li N. org. Hs. eg. db: genome wide annotation for Human. R package version 2019;2(0). 2018.
[22] Trott O, Olson AJ. AutoDock Vina: improving the speed and accuracy of docking with a new scoring function, efficient optimization, and multithreading. J Comput Chem 2010;31(2):455–61.
[23] Schrödinger L. The PyMOL molecular graphics system. 2015. Google Scholar There is no corresponding record for this reference 2018, Version 1.8.
[24] Murr C, Grammer TB, Meinitzer A, Kleber ME, März W, Fuchs D. Immune activation and inflammation in patients with cardiovascular disease are associated with higher phenylalanine to tyrosine ratios: the ludwigshafen risk and cardiovascular health study, vol. 2014. Amino Acids; 2014.
[25] Tual-Chalot S, Stellos K. Therapeutic potential of adenosine kinase inhibition in vascular disease. Cardiovasc Res 2021;117(2):354–6.
[26] Wang W, Wang B, Sun S, Cao S, Zhai X, Zhang C, Zhang Q, Yuan Q, Sun Y, Xue M. Inhibition of adenosine kinase attenuates myocardial ischaemia/reperfusion injury. J Cell Mol Med 2021;25(6):2931–43.
[27] Guo W, Liu X, Li J, Shen Y, Zhou Z, Wang M, Xie Y, Feng X, Wang L, Wu X. Prdx1 alleviates cardiomyocyte apoptosis through ROS-activated MAPK pathway during myocardial ischemia/reperfusion injury. Int J Biol Macromol 2018;112:608–15.
[28] Hu H, Nan J, Sun Y, Zhu D, Xiao C, Wang Y, Zhu L, Wu Y, Zhao J, Wu R. Electron leak from NDUFA13 within mitochondrial complex I attenuates ischemia-reperfusion injury via dimerized STAT3. Proc Natl Acad Sci USA 2017;114(45):11908–13.
[29] Jiang L, Yin X, Chen Y-H, Chen Y, Jiang W, Zheng H, Huang F-Q, Liu B, Zhou W, Qi L-W. Proteomic analysis reveals ginsenoside Rb1 attenuates myocardial ischemia/reperfusion injury through inhibiting ROS production from mitochondrial complex I. Theranostics 2021;11(4):1703.
[30] Kussmaul L, Hirst J. The mechanism of superoxide production by NADH: ubiquinone oxidoreductase (complex I) from bovine heart mitochondria. Proc Natl Acad Sci USA 2006;103(20):7607–12.
[31] Liu Y, Fiskum G, Schubert D. Generation of reactive oxygen species by the mitochondrial electron transport chain. J Neurochem 2002;80(5):780–7.
[32] Lu X, Jin Y, Wang Y, Chen Y, Fan X. Multimodal integrated strategy for the discovery and identification of quality markers in traditional Chinese medicine. J Pharm Anal 2022;12(5):701-10.
[33] Peart J, Paul Matherne G, Cerniway RJ, Headrick JP. Cardioprotection with adenosine metabolism inhibitors in ischemic–reperfused mouse heart. Cardiovasc Res 2001;52(1):120–9.
[34] Peart JN, Gross GJ. Cardioprotection following adenosine kinase inhibition in rat hearts. Basic Res Cardiol 2005;100(4):328–36.